



EM-6

## **Peristaltic Flow of Particulate Fluid Suspension through Porous Medium under the effect of Slip Conditions, Heat transfer and Magnetic Field in Catheterized Tube**

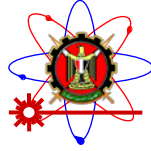
**I.M. Eldesoky<sup>(1)</sup>, W.A.El-Askary<sup>(2)</sup>, A.M. El-Refaey, M.M.Ahmed<sup>(1)</sup>**

**(1) Basic Engineering Sciences Department, Faculty of Engineering, Shebin El-Kom, Menoufiya University, Egypt**

**(2) Mechanical Power Engineering Department, Faculty of Engineering, Shebin El-Kom, Menoufiya University, Egypt**

### *Abstract*

The effect of wall slip conditions, porous media and heat transfer on peristaltic flow of MHD Newtonian fluid in catheterized tube has been studied under the assumptions of long-wavelength and low-Reynolds number. The analytical solution has been derived for velocity and temperature. The amplitude ratio ( $\varphi$ ), particle concentration ( $C$ ), catheter size ( $\epsilon$ ) and the dimensionless flow rate ( $Q$ ) were used to obtain the pressure gradient. The results for velocity and temperature obtained in the analysis have been evaluated numerically and discussed. The tube surface was maintained at a constant temperature. The variations of several parameters were discussed by using suitable graphs. The mathematical model was corresponding to the flow in the annular space of two concentric tubes.



## Introduction

The peristaltic transport through tubes /channels has attracted considerable attention due to their wide applications in medical and engineering sciences, such as urine transport from kidney to bladder, in movement of ovum in the fallopian tubes, in passage of food through esophagus and many others. In industrial applications, these flows occur in blood pumps in heart lung machine, in sanitary fluid transport and transport of corrosive fluids. It is clear the peristaltic transport of two immiscible viscous fluids in circular tube which has been studied by Ramachandra and Usha[1]. Takabatake et al. [2] has investigated peristaltic pumping in circular tubes with numerical study of fluid transport and its efficiency.

The theory of fluid suspension is very important in various situations such as sedimentation, combustion, powder technology, aerosol filtration, lunar ash flow, fluidization, atmospheric fallout, environmental pollution, etc. Most recently, the interest has developed in applying the theory of particle-fluid suspension to physiological flows including the vasomotion of small blood vessels such as arterioles, venules and capillaries [3-6].



Since the pioneering works of Latham [7] and Shapiro et al. [8] much has been said about the peristaltic flows. The study of slip flow through porous medium has attracted much attention recently. It is well known that flow through a porous medium has practical applications especially in geophysical fluid dynamics. Examples of natural porous media are beach sand, sandstone, limestone, rye bread, wood, the human lung, bile duct, gall bladder with stones and in small blood vessels. In some pathological situations, the distribution of fatty cholesterol and artery clogging blood clots in the lumen of coronary artery can be considered as equivalent to a porous medium. There are many researches about the porous media such as the influence of compliant wall properties on peristaltic motion in two-dimensional channel was noticed by Abd Elnaby and Haroun [9]. Muthu et al. [10] have analyzed the peristaltic motion of micropolar fluid in circular cylindrical tubes with elastic wall properties. El Shehawey et al. [11] investigated peristaltic transport through a porous medium. Srinivas et al. [12] studied the effect of slip conditions and porous media on peristaltic flow. Hayat et al. [13] have investigated the MHD peristaltic channel flow of a Jeffrey fluid with compliant walls and porous medium. Slip-flow was demonstrated experimentally by Derek et al. [14]. Hron et al. [15] have presented analytical solutions for the flows of a generalized fluid of complexity two in

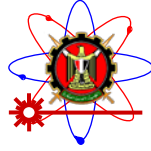


special geometries under the assumption that the slip conditions at the boundary affect on the flow. The boundary conditions of Newtonian fluid on peristaltic motion have been considered by Kwang and Fang [16]. The magneto hydrodynamic (MHD) flow of a fluid in a tube with peristalsis has interest in connection with certain problems of the movement of conductive physiological fluids, the blood, blood pump machines and with the need for theoretical research on the operation of a peristaltic MHD compressor. Effect of a moving magnetic field on blood flow was studied by Sud et al. [17], and they observed that the effect of suitable moving magnetic field accelerates the speed of blood. Ebaid [18] studied the effects of magnetic field and wall slip conditions on the peristaltic transport of a Newtonian fluid in an asymmetric channel. The interaction of peristalsis with heat transfer plays a very important role in our life. Radhakrishnamacharya et al. [19] studied the effect of heat transfer on the motion of a viscous incompressible Newtonian fluid in a channel with wall effects. Nadeem and Akbar [20] have investigated the MHD peristaltic flow of an incompressible Newtonian fluid in a uniform channel with variable viscosity in the presence of heat transfer analysis. Kothandapani and Srinivas [21] have discussed the influence of elasticity of the flexible walls on the peristaltic motion of a MHD fluid in a porous medium with heat transfer. Radhakrishnamacharya



and Srinivasulu[22] showed the influence of wall properties on peristaltic transport with heat transfer. Taneja and Jain [23] have discussed the problem of an MHD free convection flow in the presence of a temperature dependent heat source in a viscous incompressible fluid between a long vertical wavy wall and a parallel flat wall with constant heat flux and slip flow boundary condition.

To discover the real reasons of diseases in the human body, we use the endoscope theory. Thus the catheters have an important role in modifying the pressure gradient and the discovery of these reasons in different situations such as small intestines and stomach. It has become a standard tool for diagnosis and treatment of certain cardiovascular diseases in modern medicine. Vajravelu et al. [24] noted the peristaltic flow and heat transfer in a vertical porous annulus, with long wave approximation. Mekheimer and Abdelmaboud [25] studied the influence of heat transfer and magnetic field on peristaltic transport of a Newtonian fluid in a vertical annulus as an application of an Endoscope. The purpose of the present paper is to provide such an attempt for MHD Newtonian fluid through porous medium. The features of flow characteristics are analyzed by plotting graphs. The paper has been organized as follows. In Section 1, the problem is first modeled and the non-dimensional governing equations are formulated. Section 2 includes the solution of the problem under the long-



wavelength and low-Reynolds number assumptions. Numerical results and discussion are presented in Section 3. The conclusions have been summarized in Section 4.

### Mathematical Formulation

Impose the flow of a Newtonian viscous fluid through a two-dimensional symmetrical circular tube of radius  $a$ . The walls of the tube are considered to be flexible and are taken as a stretched membrane, on which traveling sinusoidal waves of moderate amplitude are imposed. A rigid catheter of radius  $a_1$  is symmetrically implemented. The flow is caused by the imposed sinusoidal wave on the compliant wall of tube. The wave shapes can be written as:

$$H(z', t') = a + b \sin\left(\frac{2\pi}{\lambda}(z' - c_w t')\right) \quad (1)$$

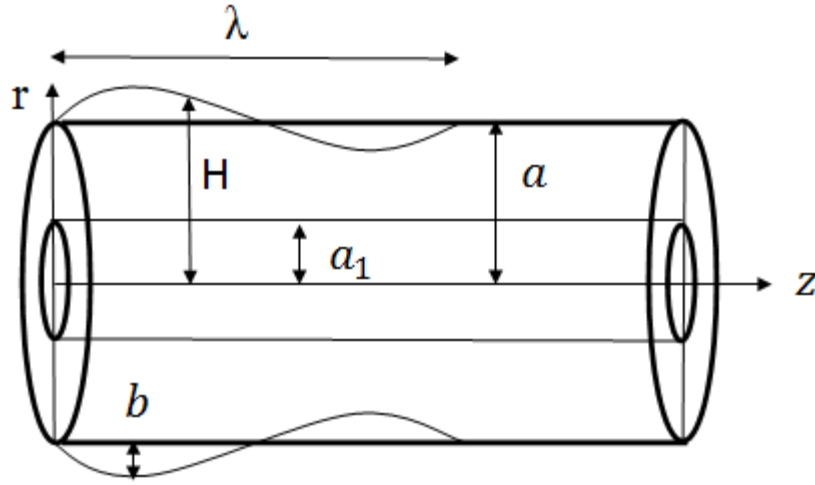


**Fig. 1, Geometry of the problem**

where  $b$  ( $0 \leq b \leq (a-a_1)$ ) is the amplitude of the wave,  $\lambda$  ( $\leq L$ , the length of the tube under consideration) is the wavelength,  $c_w$  is the wave propagation speed,  $t'$  is the time and  $z'$  is the axial coordinate. The momentum, continuity and energy equations for both the fluid and particle phases are applied on the mathematical model as expressed in [23] and [24], neglecting the inertia force of the particles and can be written as:

Axial momentum (fluid)

$$(1-C)\rho_f \left[ \frac{\partial u'_f}{\partial t'} + u'_f \frac{\partial u'_f}{\partial z'} + v'_f \frac{\partial u'_f}{\partial r'} \right] = -(1-C) \frac{\partial p'}{\partial z'} - \sigma \beta_o^2 u'_f - \frac{\mu_o}{K} u'_f +$$

$$(1-C)\mu_s(C) \left( \frac{1}{r'} \frac{\partial}{\partial r'} \left( r' \frac{\partial u'_f}{\partial r'} \right) + \frac{\partial}{\partial z'} \left( \frac{\partial u'_f}{\partial z'} \right) \right) + CS'(u'_p - u'_f), \quad (2)$$

Radial momentum (fluid)



$$(1-C)\rho_f \left[ \frac{\partial v'_f}{\partial t'} + u'_f \frac{\partial v'_f}{\partial z'} + v'_f \frac{\partial v'_f}{\partial r'} \right] = -(1-C) \frac{\partial p'}{\partial r'} +$$

$$(1-C)\mu_s(C) \left( \frac{1}{r'} \frac{\partial}{\partial r'} \left( r' \frac{\partial v'_f}{\partial r'} \right) - \frac{v'_f}{r'^2} + \frac{\partial}{\partial z'} \left( \frac{\partial v'_f}{\partial z'} \right) \right) + CS'(v'_p - v'_f), \quad (3)$$

Mass equation (fluid)

$$\frac{1}{r'} \frac{\partial}{\partial r'} (r'(1-C)v'_f) + \frac{\partial}{\partial z'} ((1-C)u'_f) = 0, \quad (4)$$

Axial momentum (particle)

$$C\rho_p \left[ \frac{\partial u'_p}{\partial t'} + u'_p \frac{\partial u'_p}{\partial z'} + v'_p \frac{\partial u'_p}{\partial r'} \right] = -C \frac{\partial p'}{\partial z'} + CS'(u'_f - u'_p), \quad (5)$$

Radial momentum (particle)

$$C\rho_p \left[ \frac{\partial v'_p}{\partial t'} + u'_p \frac{\partial v'_p}{\partial z'} + v'_p \frac{\partial v'_p}{\partial r'} \right] = -C \frac{\partial p'}{\partial r'} + CS'(v'_f - v'_p), \quad (6)$$

Mass equation (particle)

$$\frac{1}{r'} \frac{\partial}{\partial r'} (r'Cu'_p) + \frac{\partial}{\partial z'} (Cu'_p) = 0, \quad (7)$$

The energy equation can be expressed as:

$$(1-C)c_p \left[ \frac{\partial T}{\partial t'} + v'_r \frac{\partial T}{\partial r'} + v'_z \frac{\partial T}{\partial z'} \right] = \frac{K}{\rho} \left[ \frac{\partial^2 T}{\partial r'^2} + \frac{1}{r'} \frac{\partial T}{\partial r'} + \frac{\partial^2 T}{\partial z'^2} \right] +$$

$$(1-C) \frac{\mu_s}{\rho} \left( 2 \left( \left( \frac{\partial v'_r}{\partial r'} \right)^2 + \left( \frac{\partial v'_z}{\partial z'} \right)^2 + \left( \frac{v'_r}{r'} \right)^2 \right) + \left( \frac{\partial v'_r}{\partial z'} + \frac{\partial v'_z}{\partial r'} \right)^2 \right), \quad (8)$$





where  $u'$  and  $v'$  are the velocity components,  $\mu$  is the coefficient of dynamic viscosity,  $T$  is the temperature,  $c_p$  is the specific heat at constant pressure,  $K$  is the thermal conductivity and  $z'$  is the axial coordinate.

The boundary conditions that must be satisfied by the fluid on the wall and the catheter are the slip conditions suggested by Kwang and Fang [16]. They can be written as:

$$u'_w = \pm A \frac{\partial u'_w}{\partial r'} - 1, \text{ at } r' = a_1 \text{ and } r' = a + b \sin\left(\frac{2\pi}{\lambda}(z' - c_w t')\right), \quad (9)$$

$$v'_w = \pm \frac{\partial \eta}{\partial t'}, \quad \text{at } r' = a + b \sin\left(\frac{2\pi}{\lambda}(z' - c_w t')\right), \quad (10)$$

where  $u'_w$  and  $v'_w$  are the fluid or particle velocities in the streamwise and radial directions, respectively.

$$T = T_1, \text{ at } r' = a + b \sin\left(\frac{2\pi}{\lambda}(z' - c_w t')\right), \text{ (isothermal condition)} \quad (11)$$

$$\frac{\partial T}{\partial r'} = 0, \text{ at } r' = a_1 \text{ (adiabatic condition)} \quad (12)$$

where  $A$  is the mean free path (for liquid 0.05 to 0.15) and

$\eta(z', t') = b \sin\left(\frac{2\pi}{\lambda}(z' - c_w t')\right)$ ,  $r'$  is the radial coordinate,  $(u'_f, v'_f)$  denotes the

fluid phase and  $(u'_p, v'_p)$  denotes the particle phase velocity components along

$(z', r')$  directions, respectively.  $C$  is the volume fraction of particulate phase;  $\rho_f$



and  $\rho_p$  are the actual densities of the material constituting fluid and particulate phases, respectively,  $p'$  denotes the pressure,  $\mu_s(C)$  is the mixture viscosity and  $S'$  being the drag coefficient of interaction. The volume fraction density,  $C$  of the particles is chosen to be a constant which is a good approximation for the low concentration of small particles.

An empirical relation for the suspension viscosity ( $\mu_s$ ) has been chosen for the present problem as [27]:

$$\mu_s(C) = \frac{\mu_o}{1 - mC}, \quad (13)$$

where  $m = 0.07 \exp \left[ 2.49C + \left( \frac{1107}{T} \right) \exp(-1.69C) \right]$ ,  $\mu_o$  is the fluid viscosity (suspending medium) and  $T$  is the temperature of the mixture measured in absolute scale (K). The viscosity of the suspension expressed by this formula (eq. (13)) is found to be reasonably accurate up to  $C=0.59$  (i.e., 59% particle concentration)[27].

The expression for the drag coefficient of interaction  $S'$  is selected from Tam [28] as:

$$S' = \frac{9}{2} \frac{\mu_o}{a_o^2} D, \quad \text{where } D = \left[ \frac{4 + 3 \left[ 8C - 3C^2 \right]^{1/2} + 3C}{[2 - 3C]^2} \right], \quad (14)$$



with  $a_o$  as the radius of a particle.

Introducing the following dimensionless

$$\text{variables } r = \frac{r'}{a}, z = \frac{z'}{\lambda}, u_f = \frac{u'_f}{c_w}, v_f = \frac{\lambda v'_f}{ac_w}, u_p = \frac{u'_p}{c_w}, v_p = \frac{\lambda v'_p}{ac_w}, S = \frac{S'a^2}{\mu_o},$$

$$\mu = \frac{\mu_s}{\mu_o}, t = \frac{c_w t'}{\lambda}, P = \frac{a^2 P'}{\lambda c_w \mu_o}, k = \frac{K}{a^2}, \theta = \frac{(T - T_o)}{T_o}$$

and  $\text{Kn} = \frac{A}{a}$ , where Kn is knudsen number,  $\theta$  is the dimensionless temperature

and  $k$  is the dimensionless thermal conductivity.

Substituting the dimensionless parameters into the governing equations (2)-(12), yields the followings:

$$(1-C)\delta \text{Re} \left( \frac{\partial u_f}{\partial t} + u_f \frac{\partial u_f}{\partial z} + v_f \frac{\partial u_f}{\partial r} \right) = -(1-C) \frac{\partial p}{\partial z} - \left( \frac{\sigma \beta_o^2 a^2}{\mu_o} + \frac{1}{k} \right) u_f$$

$$(1-C)\mu \left( \frac{1}{r} \frac{\partial}{\partial r} \left( r \frac{\partial u_f}{\partial r} \right) + \delta^2 \frac{\partial}{\partial z} \left( \frac{\partial u_f}{\partial z} \right) \right) + CS(u_p - u_f), \quad (15)$$

$$(1-C)\delta \text{Re} \left( \frac{\partial v_f}{\partial t} + u_f \frac{\partial v_f}{\partial z} + v_f \frac{\partial v_f}{\partial r} \right) = -(1-C) \frac{\partial p}{\partial r} +$$

$$(1-C)\mu \delta^2 \left( \frac{\partial}{\partial r} \frac{1}{r} \left( \frac{\partial (rv_f)}{\partial r} \right) - \frac{1}{r^2} + \delta^2 \frac{\partial}{\partial z} \left( \frac{\partial v_f}{\partial z} \right) \right) + CS(v_p - v_f), \quad (16)$$



$$\frac{1}{r} \frac{\partial}{\partial r} (r(1-C)v_f) + \frac{\partial}{\partial z} ((1-C)u_f) = 0, \quad (17)$$

$$C \frac{\rho_p}{\rho_f} \text{Re} \delta \left( \frac{\partial u_p}{\partial t} + u_p \frac{\partial u_p}{\partial z} + v_p \frac{\partial u_p}{\partial r} \right) = -C \frac{\partial p}{\partial z} + CS (u_f - u_p), \quad (18)$$

$$C \frac{\rho_p}{\rho_f} \text{Re} \delta \left( \frac{\partial v_p}{\partial t} + u_p \frac{\partial v_p}{\partial z} + v_p \frac{\partial v_p}{\partial r} \right) = -C \frac{\partial p}{\partial r} + CS \delta^2 (v_f - v_p), \quad (19)$$

$$\frac{1}{r} \frac{\partial}{\partial r} (rCv_p) + \frac{\partial}{\partial z} (Cu_p) = 0, \quad (20)$$

$$(1-C) \delta \text{Re} \left( \frac{\partial \theta}{\partial t} + v_r \frac{\partial \theta}{\partial r} + v_z \frac{\partial \theta}{\partial z} \right) = \frac{k}{c_p \mu_0} \left( \frac{\partial^2 \theta}{\partial r^2} + \frac{1}{r} \frac{\partial \theta}{\partial r} + \delta^2 \frac{\partial^2 \theta}{\partial z^2} \right) +$$

$$(1-C) \frac{\mu c^2}{c_p T_o} \left( 2\delta^2 \left( \frac{\partial v_r}{\partial r} \right)^2 + 2\delta^2 \left( \frac{\partial v_z}{\partial z} \right)^2 + 2\delta^2 \left( \frac{v_r}{r} \right)^2 + \delta^4 \left( \frac{\partial v_r}{\partial z} \right)^2 + \left( \frac{\partial v_z}{\partial r} \right)^2 + 2\delta^2 \frac{\partial v_r}{\partial z} \frac{\partial v_z}{\partial r} \right), \quad (21)$$

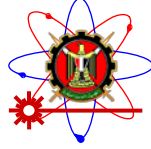
The amplitude equation will be dimensionlized to become:

$$h = 1 + \phi \sin(2\pi z).$$

The dimensionless parameters in the previous equations are:  $\text{Re} = \rho_f c_w a / \mu_o$ ,

$\delta = a / \lambda$  and  $\varphi = \frac{b}{a}$ ,  $\varepsilon = a_1 / a$ ,  $M = \sqrt{\sigma / \mu_o} \beta_o a$ , where Re =Reynolds number,  $\delta$ =wave

number,  $\varphi$ =amplitude ratio,  $\varepsilon$  =catheter size and  $M$  =magnetic parameter, respectively.



Using the long wavelength approximation (i.e.,  $\delta \ll 1$ ) as considered in Shapiro et al. [8], the equations describing the flow in the wave frame can be reduced to:

Reduced radial momentum equation of particle

$$\frac{dp}{dr} = 0, \quad (22)$$

Reduced radial momentum equation of fluid

$$(1-C) \frac{dp}{dr} = CS (v_p - v_f), \quad (23)$$

$$v_p = v_f = 0 \text{ at } r = \varepsilon,$$

$$v_p = v_f \neq 0 \text{ at } r = h.$$

Reduced axial momentum equation of fluid

$$(1-C) \frac{dp}{dz} = (1-C) \frac{\mu}{r} \frac{\partial}{\partial r} \left( r \frac{\partial u_f}{\partial r} \right) - \left( M^2 + \frac{1}{k} \right) u_f + CS (u_p - u_f). \quad (24)$$

Reduced axial momentum equation of particle

$$C \frac{dp}{dz} = CS (u_f - u_p). \quad (25)$$

Reduced energy equation

$$-\frac{k}{c_p \mu_o} \left( \frac{\partial^2 \theta}{\partial r^2} + \frac{1}{r} \frac{\partial \theta}{\partial r} \right) = (1-C) \frac{\mu c_w^2}{c_p T_o} \left( \frac{\partial v_z}{\partial r} \right)^2. \quad (26)$$

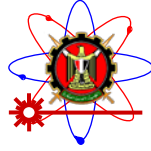
The non dimensional slip and temperature conditions are:

$$u_f = \pm k_n \frac{\partial u_f}{\partial r} - 1, \text{ at } r = \varepsilon, \quad (27)$$

$$u_f = \pm k_n \frac{\partial u_f}{\partial r} - 1, \text{ at } r = h = 1 + \phi \sin(2\pi z), \quad (28)$$

$$\theta_f = \theta_1 = 1, \text{ at } r = h = 1 + \phi \sin(2\pi z), \quad (29)$$

$$\frac{\partial \theta}{\partial r} = 0, \text{ at } r = \varepsilon. \quad (30)$$



The expressions for the velocity profiles,  $u_f$  and  $u_p$ , obtained as the solution of the equations (24) and (25), subjected to the boundary conditions (27) and (28) are:

$$u_f = \frac{\frac{(dP / dz)}{(1-C)\mu}}{-(M^2 + \frac{1}{k})} + n_1 b r_1 + m_1 b r_2, \quad (31)$$

$$\frac{dp}{dz} = \frac{-8\mu(1-C) \left( Q - 1 - \frac{\phi^2}{2} + h^2 \right)}{(h^2 - \varepsilon^2) X_z} \quad (32)$$

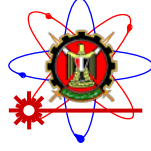
where  $n_1, m_2, d, X_z, \beta$  are

$$n_1 = \frac{d(b\varepsilon_2 - k_n q_6) - d(b h_2 - k_n q_4)}{(b h_1 - k_n q_3)(b\varepsilon_2 - k_n q_6) - (b h_2 - k_n q_4)(b\varepsilon_1 - k_n q_5)}$$

$$m_1 = \frac{d(b h_1 - k_n q_3) - d(b\varepsilon_1 - k_n q_5)}{(b h_1 - k_n q_3)(b\varepsilon_2 - k_n q_6) - (b h_2 - k_n q_4)(b\varepsilon_1 - k_n q_5)}$$

$$d = -1 + \frac{\frac{(dp / dz)}{(1-C)\mu}}{M^2 + \frac{1}{k}}, X_z = h^2 + \varepsilon^2 + \beta - \frac{(h^2 - \varepsilon^2)}{\ln(\frac{h}{\varepsilon})}, \beta = \frac{8\mu C(1-C)}{S}$$

From which,



$$br_1 = I_0(r) = 1 + \frac{g^2 r^2}{4} + \frac{g^4 r^4}{64}$$

$$br_2 = K_0(r) = -\ln\left(\frac{g \cdot r}{2}\right) - \frac{g^2 r^2 \ln\left(\frac{g \cdot r}{2}\right)}{4} + \frac{(2-2\gamma)g^2 r^2}{8} - \gamma$$

$$bh_1 = I_0(h), bh_2 = K_0(h), b\varepsilon_1 = I_0(\varepsilon), b\varepsilon_2 = K_0(\varepsilon),$$

$$q_3 = \frac{\partial bh_1}{\partial h}, q_4 = \frac{\partial bh_2}{\partial h}, q_5 = \frac{\partial b\varepsilon_1}{\partial \varepsilon}, q_6 = \frac{\partial b\varepsilon_2}{\partial \varepsilon}, g = \sqrt{\left(M^2 + \frac{1}{k}\right)},$$

$I_0$  is the modified Bessel function at zero order of the first kind

$K_0$  is the modified Bessel function at zero order of the second kind

The expression for the temperature profiles,  $\theta$  obtained as the solution of the equation (26), with introducing the temperature conditions (29),(30)is:

$$\theta = C_1 + C_2 \ln(r) - (1-C)\mu B_r T_p \quad (37)$$

where



$$\begin{aligned}
 T_p &= a[b(\frac{g^4 r^3}{36} + \frac{g^8 r^7}{16^2 \cdot 49} + \frac{g^6 r^5}{16.25}) + \frac{1}{r} + \frac{g^4 r^3}{16.9} + \frac{g^4 r^3}{36} (\ln \frac{g}{2})^2 + \frac{g^4 r^3}{36} ((\ln r)^2 - \frac{4r}{3} \ln r + \frac{2}{3}) \\
 &+ \frac{g^4 r^3}{18} \ln(\frac{g}{2})(\ln r - \frac{2}{3}) + \frac{g^4 r^3}{16.9} (2 - 2\gamma) - \frac{g^4 r^3}{36} ((2 - 2\gamma) + 1)(\ln \frac{g}{2} + \ln r - \frac{2}{3}) - \frac{g^4 r^3}{8.9} (2 - 2\gamma) \\
 &+ g^2 r (\ln \frac{g}{2} + \ln r - 2) + \frac{g^2 r}{2} (1 - (2 - 2\gamma)) - 2\sqrt{b} (-\frac{g^2 r}{2} - \frac{g^4 r^3}{16.9} - \frac{g^4 r^3}{8.9} + \frac{g^6 r^5}{64.25} - \\
 &\frac{g^4 r^3}{36} (\ln \frac{g}{2} + \ln r - \frac{2}{3}) - \frac{g^6 r^5}{32.25} (\ln \frac{g}{2} + \ln r - \frac{2}{3}) + \frac{g^4 r^3}{8.9} (2 - 2\gamma) + \frac{g^6 r^5}{64.25} (2 - 2\gamma)) \\
 C_1 &= \theta_1 - C_2 \ln h + (1 - C) \mu B_r a [b(\frac{g^4 h^3}{36} + \frac{g^8 h^7}{16^2 \cdot 49} + \frac{g^6 h^5}{16.25}) + \frac{1}{h} + \frac{g^4 h^3}{16.9} + \frac{g^4 h^3}{36} (\ln \frac{g}{2})^2 + \frac{g^4 h^3}{36} ((\ln h)^2 - \frac{4h}{3} \ln h + \frac{2}{3}) \\
 &+ \frac{g^4 h^3}{18} \ln(\frac{g}{2})(\ln h - \frac{2}{3}) + \frac{g^4 h^3}{16.9} (2 - 2\gamma) - \frac{g^4 h^3}{36} ((2 - 2\gamma) + 1)(\ln \frac{g}{2} + \ln h - \frac{2}{3}) - \frac{g^4 h^3}{8.9} (2 - 2\gamma) \\
 &+ g^2 h (\ln \frac{g}{2} + \ln h - 2) + \frac{g^2 h}{2} (1 - (2 - 2\gamma)) - 2\sqrt{b} (-\frac{g^2 h}{2} - \frac{g^4 h^3}{16.9} - \frac{g^4 h^3}{8.9} + \frac{g^6 h^5}{64.25} - \\
 &\frac{g^4 h^3}{36} (\ln \frac{g}{2} + \ln h - \frac{2}{3}) - \frac{g^6 h^5}{32.25} (\ln \frac{g}{2} + \ln h - \frac{2}{3}) + \frac{g^4 h^3}{8.9} (2 - 2\gamma) + \frac{g^6 h^5}{64.25} (2 - 2\gamma)) \\
 C_2 &= (1 - C) \mu B_r \varepsilon a [b(\frac{g^4 r^2}{12} + \frac{g^8 r^6}{16^2 \cdot 7} + \frac{g^6 r^4}{16.5}) - \frac{1}{r^2} + \frac{g^4 r^2}{16.3} + \frac{g^4 r^2}{12} (\ln \frac{g}{2})^2 + \frac{g^4}{36} (2r^2 \ln r + (\ln r)^2 3r^2 - \frac{4}{3} (r^2 + 3r^2 \ln r) + 2r^2) \\
 &+ \frac{g^4}{18} \ln(\frac{g}{2})(r^2 + 3r^2 \ln r - 2r^2) + \frac{g^4 r^2}{16.3} (2 - 2\gamma)^2 - \frac{g^4}{4} ((2 - 2\gamma) + 1)(\frac{r^2}{3} \ln \frac{g}{2} + \frac{1}{9} (r^2 + 3r^2 \ln r - 2r^2)) - \frac{g^4 r^2}{8.3} (2 - 2\gamma) \\
 &+ g^2 (\ln \frac{g}{2} + \ln r - 1) + \frac{g^2}{2} (1 - (2 - 2\gamma)) - 2\sqrt{b} (-\frac{g^2}{2} - \frac{g^4 r^2}{16.3} - \frac{g^4 r^2}{8.3} + \frac{g^6 r^4}{64.5} - \\
 &\frac{g^4}{4} (\frac{r^2}{3} \ln \frac{g}{2} + \frac{1}{9} (r^2 + 3r^2 \ln r - 2r^2)) - \frac{g^6}{32} (\frac{r^4}{5} \ln \frac{g}{2} + \frac{1}{25} (r^4 + 5r^4 \ln r - 2r^4)) + (2 - 2\gamma) (\frac{g^4 r^2}{8.3} + \frac{g^6 r^4}{64.5})]
 \end{aligned}$$

where

$$a = (m_1)^2, b = (\frac{n_1}{m_1})^2, \text{Pr} = \mu_o c_p / k, E = c^2 / c_p T_o, Br = E \text{Pr}$$

in which Pr = Prandtl number,  $E$  = Echert number,  $Br$  = Brinkman number





## NUMERICAL RESULTS AND DISCUSSION

The effects of the various parameters including the particle concentration,  $C$ , the catheter size,  $\varepsilon$ , and the amplitude ratio  $\varphi$  will be discussed. The analytical results derived in the study are considered at a reference temperature of 298 K. The parameter values are chosen as:  $a$  (tube radius) = 1.25 cm;  $C=0, 0.2, 0.4$ , and  $0.59$ ;  $\varphi = 0, 0.2, 0.4$  and  $0.6$ ;  $\varepsilon = 0, 0.1, 0.2, 0.3, 0.4, 0.5$  and  $0.6$ ;  $a_p$  (radius of a particle) = 0.1 cm and  $Q=0, 0.4, 0.6, 0.8$ , and  $1.0$ . The present study includes different cases for  $C=0$  (absence of concentration) and (presence of concentration). On the other hand, the variation of amplitude ratio is taken into consideration. Also the results of the thermal study have been investigated under different values of flow rate ( $Q=0, 0.2, 0.4$ ), catheter size ( $\varepsilon=0.1, 0.2, 0.3$ ), amplitude ratio ( $\varphi=0, 0.2, 0.4$ ) and fluid suspension ( $C=0, 0.2, 0.4, 0.59$ ).

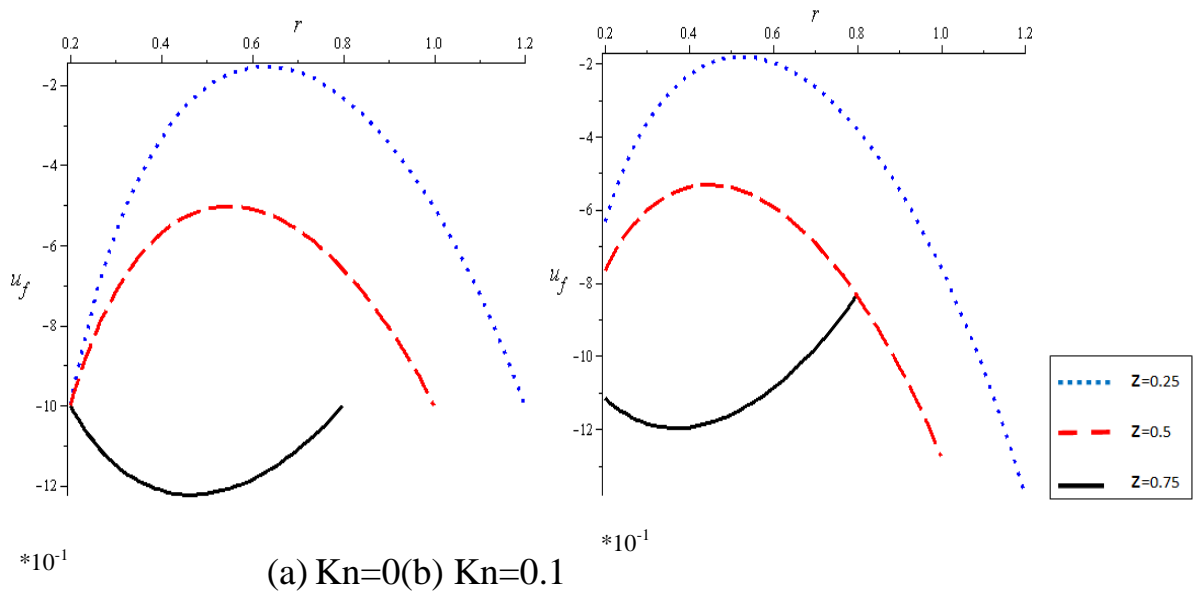


Fig. 2 Velocity profiles at different values of  $z$  for (a)  $Kn=0$  and (b)  $Kn=0.1$  at ( $\varepsilon=0.2, M=2, k=5, \varphi=0.2, Q=0.2$ ).

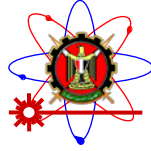


Fig. 2 shows the axial velocity profiles at different locations, in which at  $z=0.75$ , the velocity increases because of the reduced flow area and at  $z=0.25$ , the velocity decreases, due to the enlarged cross section.

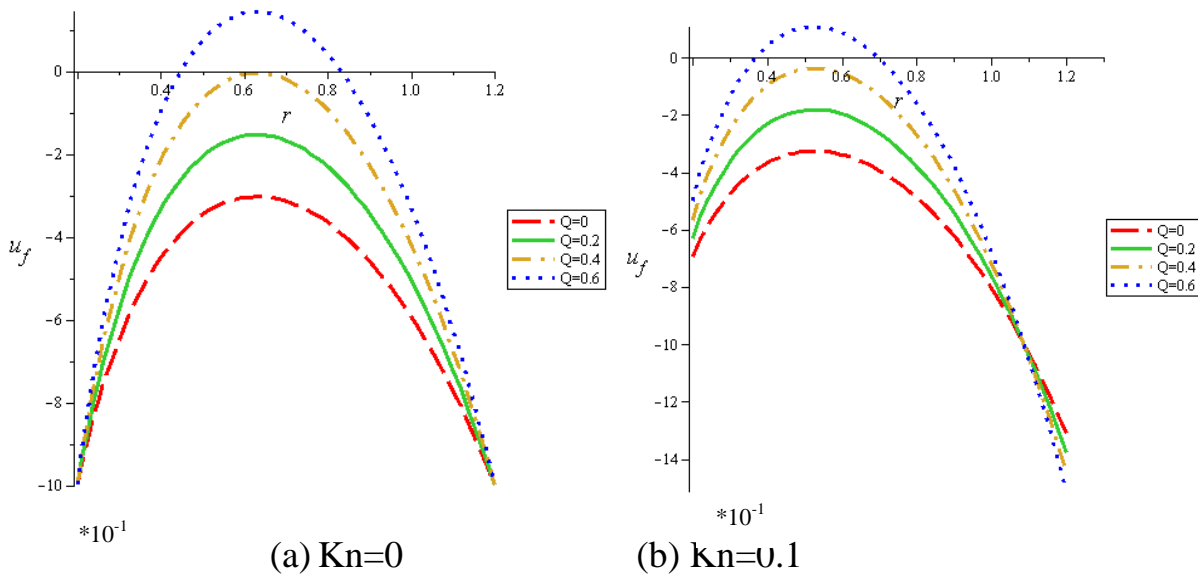


Fig. 3 Velocity profiles at different flow rates for (a)  $Kn=0$  and (b)  $Kn=0.1$  at ( $\varepsilon=0.2$ ,  $M=2$ ,  $k=5$ ,  $\varphi=0.2$ ,  $Q=0.2$ ).

Fig.3 represents the velocity profiles of the fluid at different flow rates. With the absence of catheter, the velocity profiles are seen similar with increase of the central velocity with the flow rate. The tube wall velocity increases with the flow rate in the case of catheterized tube ( $Kn=0.1$ ), while the catheter wall velocity decreases.

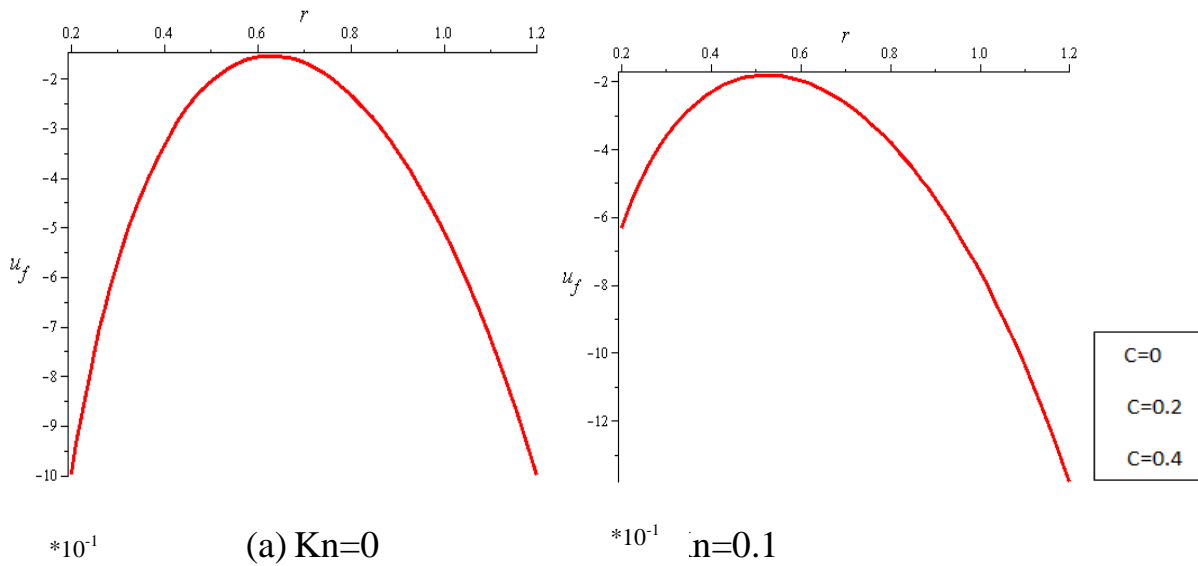
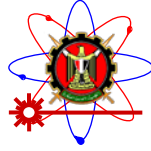
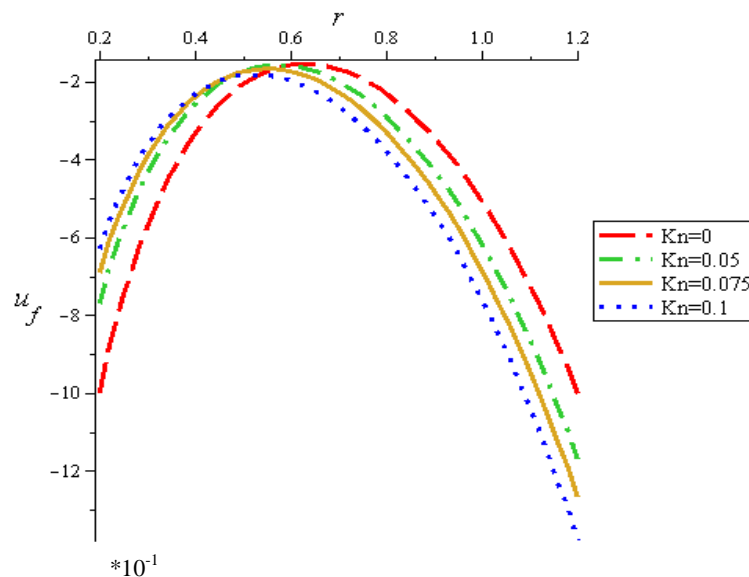


Fig. 4 Velocity profiles at different concentrations for (a)  $Kn=0$  and (b)  $Kn=0.1$  at  $(\varepsilon=0.2, M=2, k=5, \varphi=0.2, Q=0.2)$ . The effects of particles concentration on the velocity distribution at  $\varphi=0.2$ ,  $\varepsilon=0.2$ ,  $Q=0.2$  are seen in Fig. 4. For both non-slip condition and slip condition, it is noticed that different suspension has no effect on the velocity distribution.



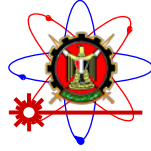


Fig. 5 Velocity profiles at different values of Knat ( $\varepsilon=0.2$ ,  $M=2$ ,  $k=5$ ,  $\varphi=0.2$ ,  $Q=0.2$ ).

Fig. 5 represents the velocity profiles of the fluid with slip condition at different Knudsen number. It is observed that slip conditions on the tube wall enhances the near-wall velocity, while slip conditions at the catheter reduces the near-wall velocity.

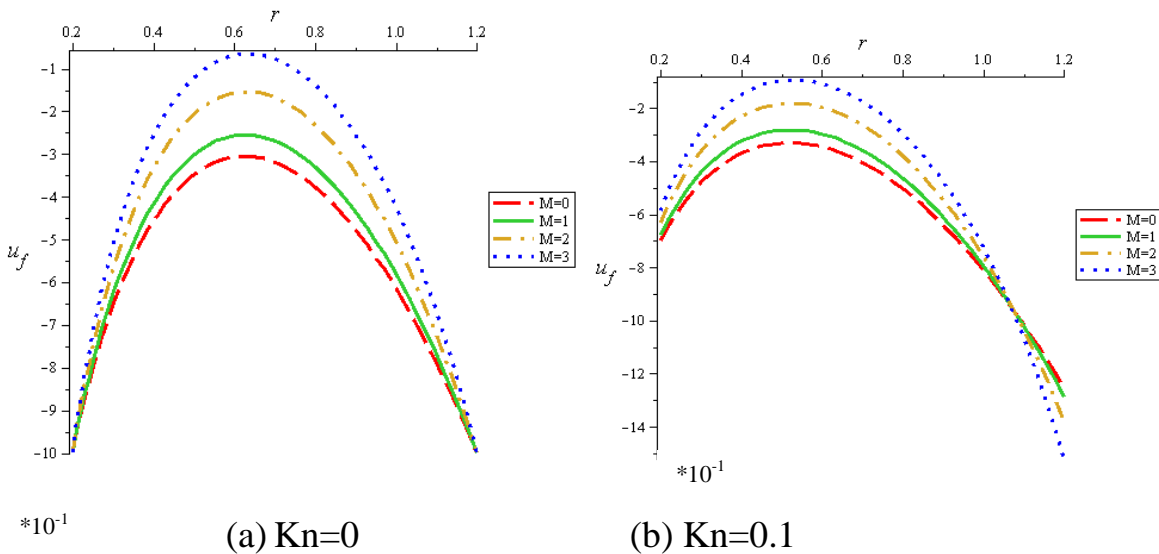


Fig. 6 Velocity profiles at different values of M for (a)  $Kn=0$  and (b)  $Kn=0.1$  at ( $\varepsilon=0.2$ ,  $C=0.2$ ,  $k=5$ ,  $\varphi=0.2$ ,  $Q=0.2$ ).

Fig. 6 shows the velocity profiles of the fluid with MHD at different magnetic fields. It is noticed that the magnetic parameter on the tube wall increases the near-wall velocity, while the near-wall velocity of the catheter decreases with magnetic parameter.

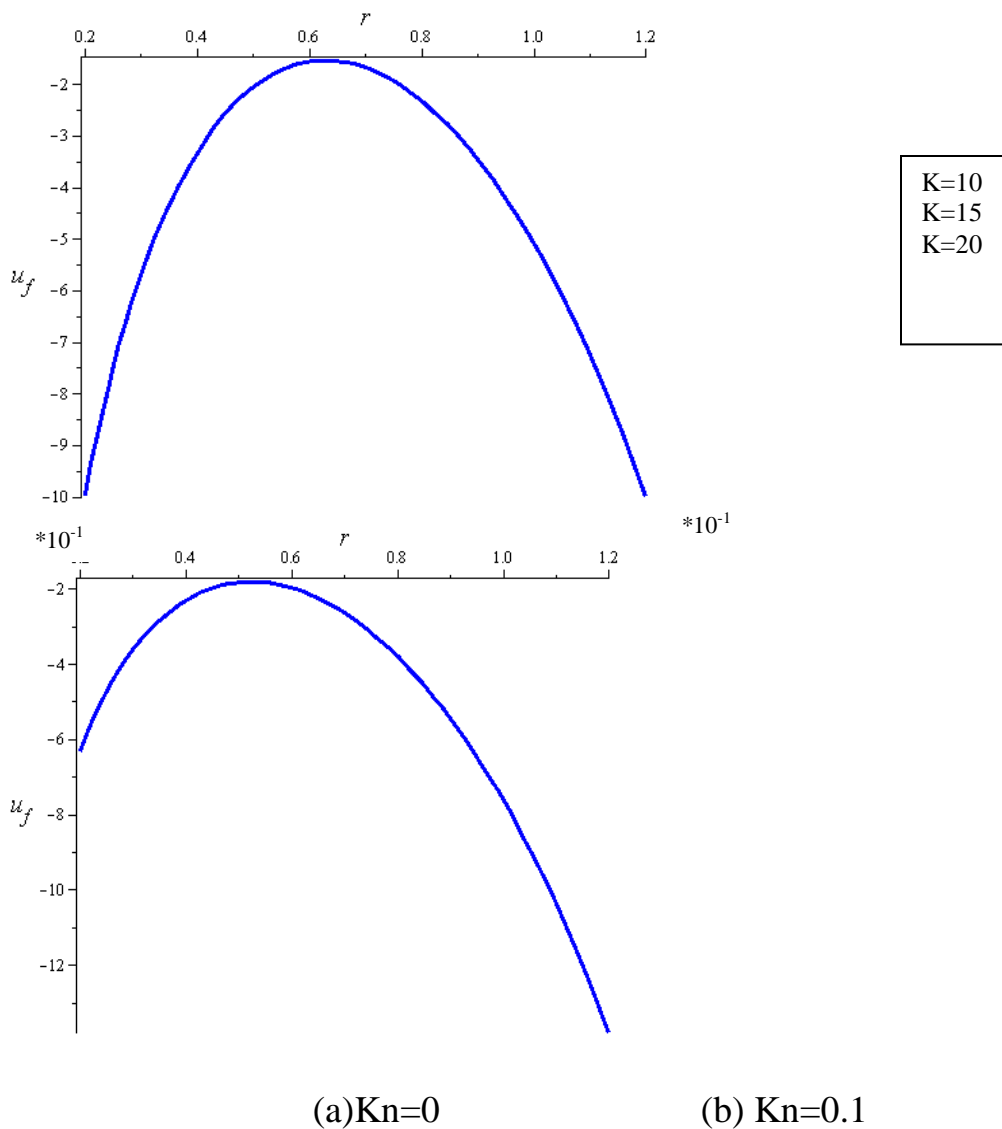


Fig. 7 Velocity profiles at different porous media for (a)  $Kn=0$  and (b)  $Kn=0.1$  at ( $\epsilon=0.2$ ,  $C=0.2$ ,  $M=2$ ,  $\varphi=0.2$ ,  $Q=0.2$ ).

Fig. 7 represents the effect of porous media on the velocity distributions for  $\varphi=0.2$ ,  $\epsilon=0.2$ ,  $Q=0.2$ . It is observed that with porous media, there is a very low effect on velocity distribution.

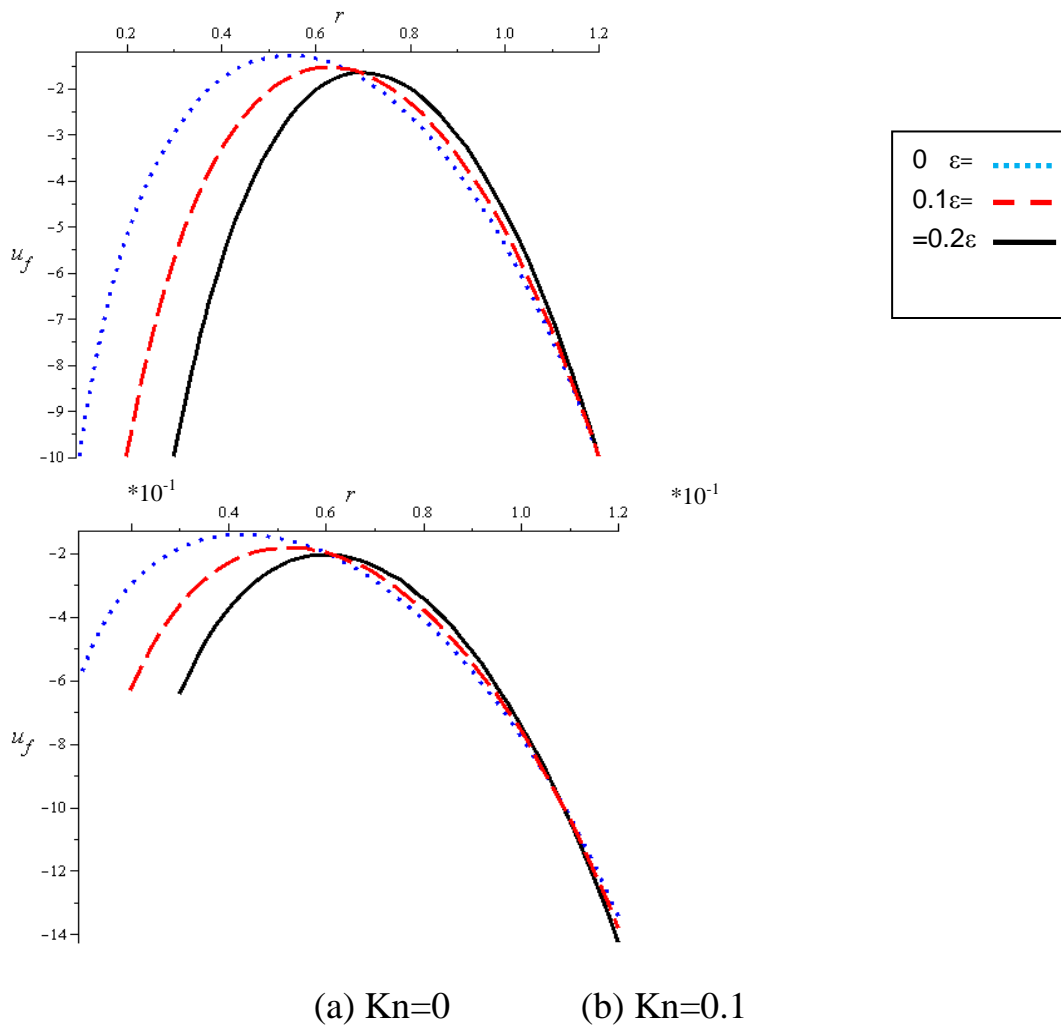
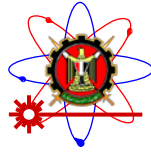


Fig. 8 Velocity profiles at different catheter sizes for (a)  $Kn=0$  and (b)  $Kn=0.1$  at ( $k=5, C=0.2, M=2, \varphi=0.2, Q=0.2$ ).

In the case of no-slip and slip conditions, the velocity increases with the catheter as noticed in Fig. 8.

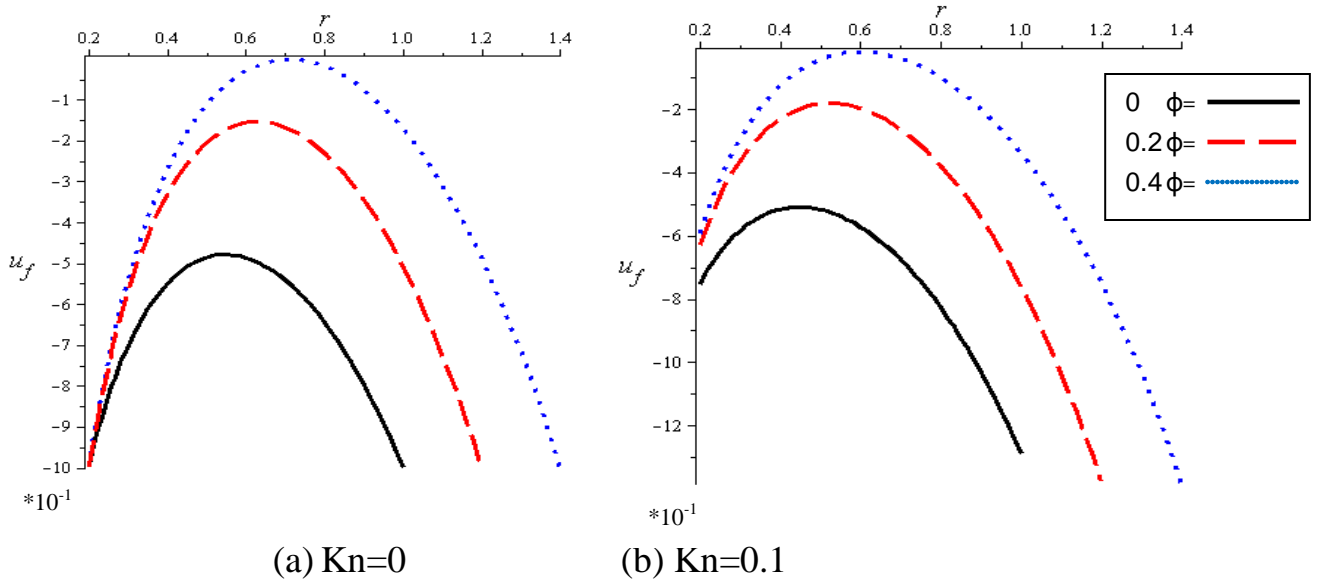
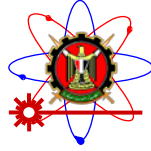


Fig. 9 Velocity profiles at different amplitude ratios for (a)  $Kn=0$  and (b)  $Kn=0.1$  at  $(k=5, C=0.2, M=2, \varepsilon=0.2, Q=0.2)$ .

The effect of amplitude ratio ( $\varphi$ ) on the velocity distribution is shown in Fig. 9, in which the velocity decreases when ( $\varphi$ ) increases.

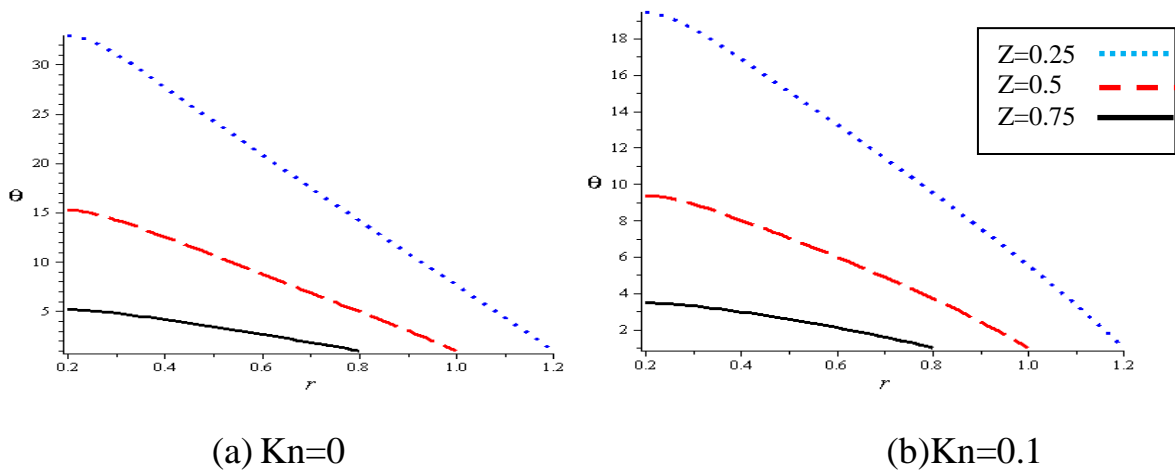


Fig. 10 Temperature profiles at different values of  $z$  for (a)  $Kn=0$  and (b)  $Kn=0.1$  at  $(k=5, C=0.2, M=2, \varepsilon=0.2, Q=0.2, \varphi=0.2)$ .

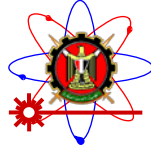
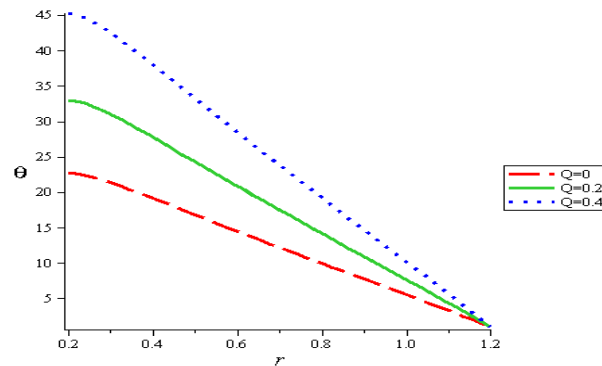
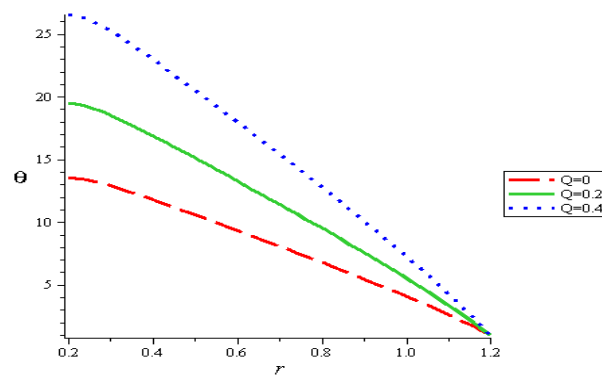


Fig. 10 shows the relation between the temperature and the radius at different locations where at the expansion ( $z=0.25$ ), temperature increases, and at the contraction ( $z=0.75$ ), temperature decreases.



(a)  $Kn=0$



(b)  $Kn=0.1$

Fig. 11 Variation of  $\theta$  with the flow rate for (a)  $Kn=0$  and (b)  $Kn=0.1$  at ( $k=5$ ,  $C=0.2$ ,  $M=2$ ,  $\varepsilon=0.2$ ,  $\varphi=0.2$ ).

The flow rate plays also an important role in enhancing the temperature ( $\theta$ ), in which with increasing the flow rate, the thermal energy increases for both without slipping and with slipping, see Fig. 11.



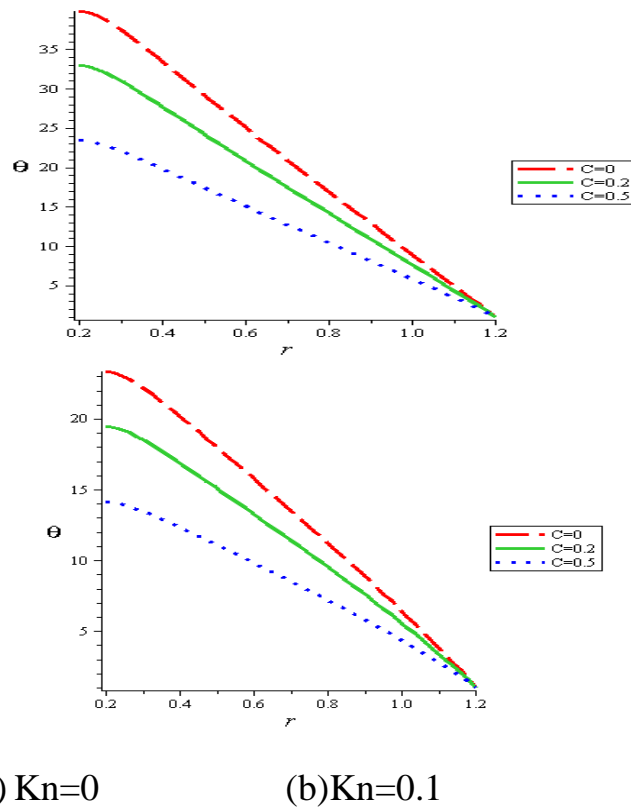


Fig. 12 Variation of  $\theta$  with suspension for (a)  $Kn=0$  and (b)  $Kn=0.1$  at ( $k=5$ ,  $C=0.2$ ,  $M=2$ ,  $\varepsilon=0.2$ ,  $\varphi=0.2$ ).

It is observed that temperature ( $\theta$ ) decreases with the presence of suspension ( $C$ ) as shown in Fig.12 for both without and with slipping.

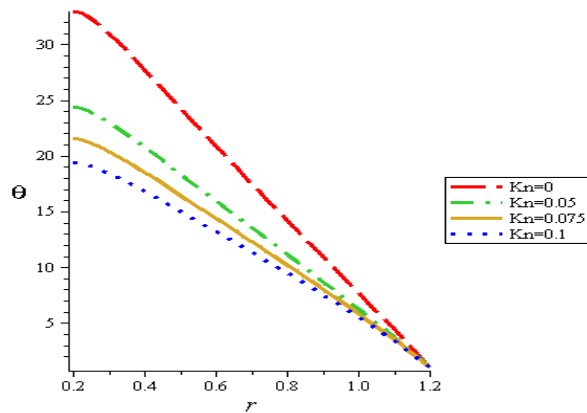


Fig.13 Temperature profiles at different values of  $Kn$ .

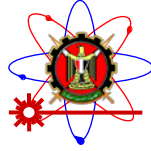
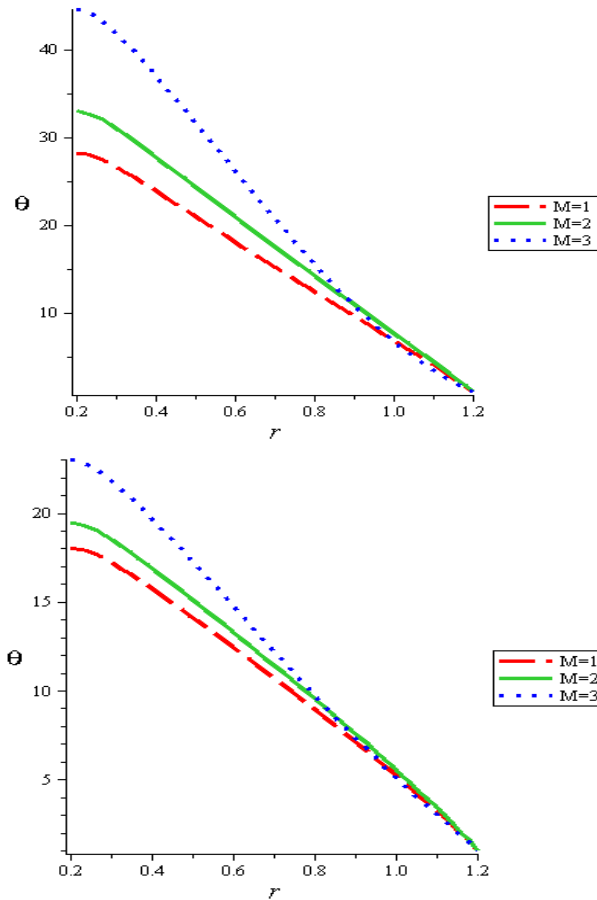


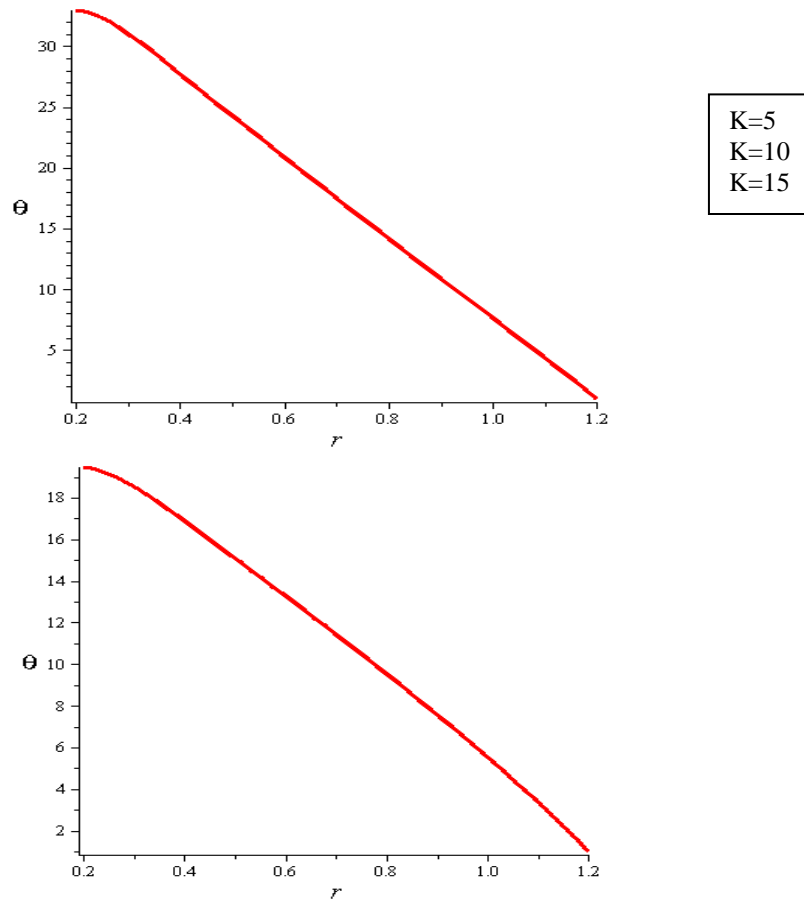
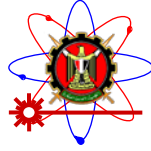
Fig. 13 shows the relation between temperature and the slip parameter at the wall and the catheter, where temperature decreases when Knudsen number increases.



(a)  $Kn=0$  (b)  $Kn=0.1$

Fig. 14 Variation of  $\theta$  with the magnetic field for (a)  $Kn=0$  and (b)  $Kn=0.1$  at ( $k=5$ ,  $C=0.2$ ,  $C=0.2$ ,  $\varepsilon=0.2$ ,  $\varphi=0.2$ ).

The temperature strongly increases with the presence of Magnetic field ( $M$ ) as shown in Fig.14, because of the enhanced thermal energy accompanied with the magnetic field.



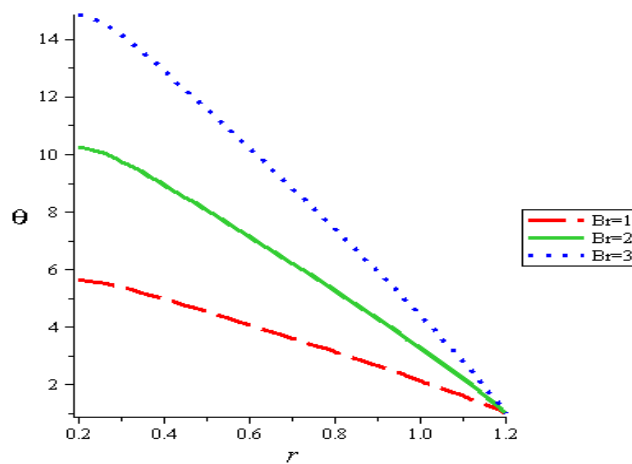
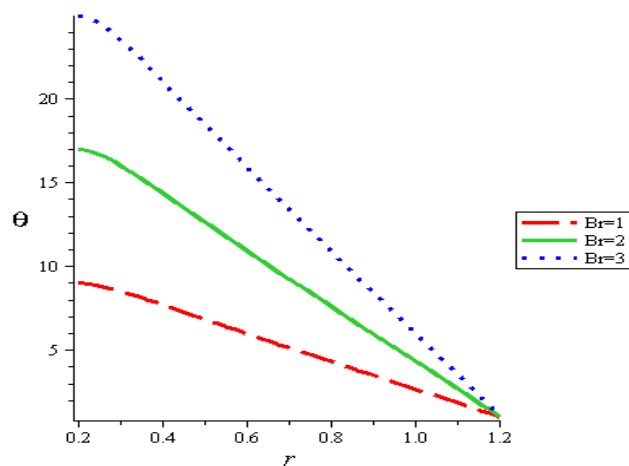
(a)  $Kn=0$

(b)  $Kn=0.1$

Fig. 15 Variation of  $\theta$  with the porous media for (a)  $Kn=0$  and (b)  $Kn=0.1$   
at  $(M=2, C=0.2, C=0.2, \varepsilon=0.2, \varphi=0.2)$ .

No variation of the temperature distribution with the presence of porous media,

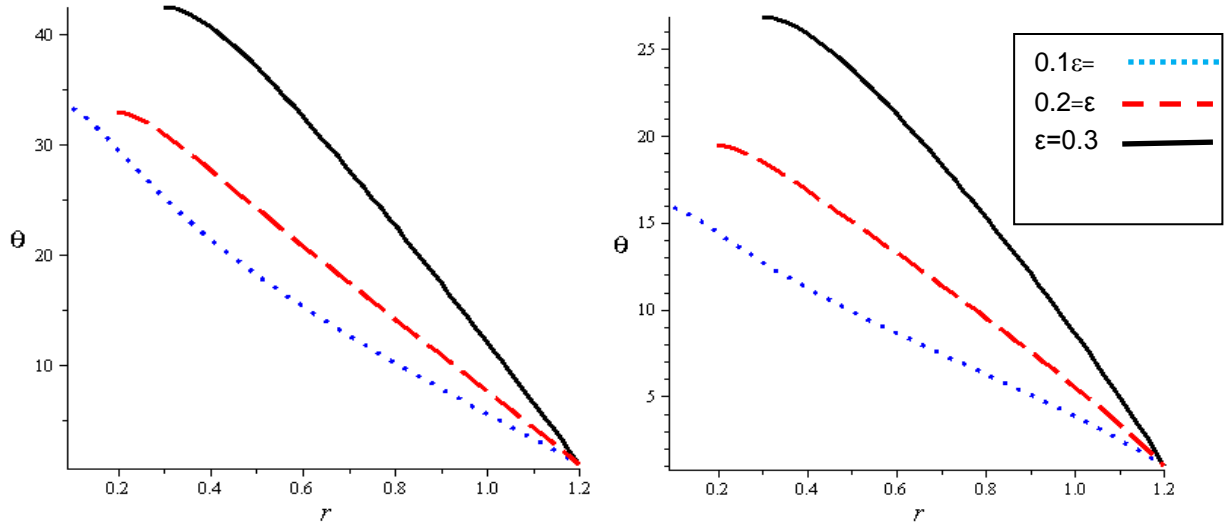
see Fig. 15.



(a) Kn=0

(b)Kn=0.1

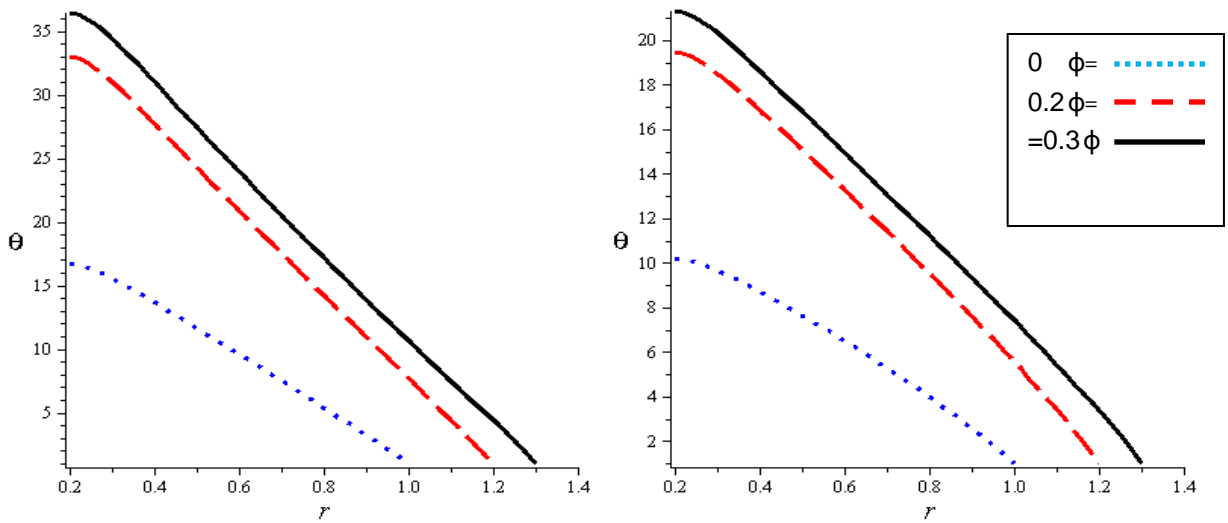
Fig. 16 Variation of  $\theta$  with the Brinkman number for (a) Kn=0 and (b)Kn=0.1 at ( $M=2$ ,  $C=0.2$ ,  $C=0.2$ ,  $\varepsilon=0.2$ ,  $\varphi=0.2$ ,  $k=5$ ).



(a) Kn=0

(b)Kn=0.1

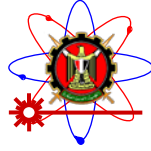
Fig. 17 Variation of  $\theta$  with the catheter size for (a) Kn=0 and (b)Kn=0.1 at ( $M=2, C=0.2, Q=0.2, \varphi=0.2, k=5$ ).



(a) Kn=0

(b)Kn=0.1

Fig. 18 Variation of  $\theta$  with the amplitude ratio for (a)Kn=0 and (b)Kn=0.1 at ( $M=2, C=0.2, Q=0.2, \varepsilon=0.2, k=5$ ).

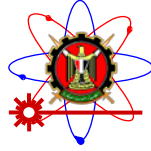


For both without and with slipping, it is observed that the temperature also increases with Brinkman number (Br) as observed from Fig. 16. Temperature increases with the presence of catheter, see Fig. 17. The effect of amplitude ratio ( $\varphi$ ) on the temperature distribution is shown in Fig. 18, in which the temperature increases when ( $\varphi$ ) increases.

### Conclusion

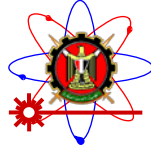
This study investigated the both effects of slip conditions and heat transfer on a particulate fluid suspension with peristaltic transport in catheterized tube under the influence of MHD and porous media. The analytical solution has been developed and used for extracting, the velocity and temperature of the fluid for uniform tube under a long wave length and low Reynolds number approximations. The features of the flow characteristics are analyzed using graphs and discussions. For both slipping and no slipping, main points are obtained from the present study:

- 1- At the contraction, velocity increases, while at the expansion, velocity decreases.
- 2- The flow rate enhances the velocity at the wall, and reduces the velocity at the catheter.
- 3- The particle concentration and porous media have no effect on the velocity.
- 4- The velocity increases with slip condition and magnetic field at the wall, while it decreases at the catheter.
- 5- The temperature decreases at the contraction, while it increases at the expansion.
- 6- The flow rate, magnetic field and the presence of catheter enhance the thermal energy of the fluid.
- 7- The particle concentration and slip condition decrease the thermal energy, while porous media has no effect on the temperature.
- 8- Brinkman number enhances the temperature.



## References

- [1] Ramachandra Rao A. and Usha S., "Peristaltic transport of two immiscible viscous fluid in a circular tube", *Journal Fluid Mechanics* 298, 271-285, 1995.
- [2] Takabatake, S., Ayukawa, K. and Mori A., "Peristaltic pumping in circular tubes: A numerical study of fluid transport and its efficiency", *Journal Fluid Mechanics* 193, 267-283, 1988.
- [3] Srivastava, L.M. and Srivastava, V.P., "Peristaltic transport of a Particle-fluid suspension", *Journal Biomechanics* 111, 157-165, 1989.
- [4] Srivastava, V. P., "Particle-fluid suspension model of blood flow through stenotic vessels with applications", *International Journal Biomechanics and Computer* 38, 141-154, 1995.
- [5] Mekheimer, Kh. S., "Peristaltic motion of a particle-fluid suspension in a planar channel", *International Journal Theoretical Physics* 37, 2895-2920, 1998.
- [6] Medhavi, A. and Singh, U. K., "A two-layered suspension flow induced by peristaltic waves", *International Journal Fluid Mechanics* 35, 258-272, 2008.
- [7] Latham, T. W., "Fluid motions in peristaltic pump", MS Thesis, MIT, Cambridge, Massachusetts, 1966.
- [8] Shapiro, A.H., Jaffrin, M. Y. and Weinberg, S.L., "Peristaltic pumping with long wavelength at low Reynolds number", 1969.
- [9] Abd Elnaby, M.A. and Haroun, M.H., "Influence of compliant wall properties on peristaltic motion in two-dimensional channel", *Communication Nonlinear Science Numerical Simulation* 13, 738-752, 2008.
- [10] Muthu, P., Rathish Kumar, B.V. and Chandra, P., "Peristaltic motion of micropolar fluid in circular cylindrical tubes with elastic wall properties", *ANZIAM Journal* 45, 232-245, 2003.
- [11] El Shehawey, E. F., Mekheimer, Kh. S., Kaldas, S. F. and Afifi N. A. S., "Peristaltic transport through a porous medium", *Journal Biomathematics* 14, 16-38, 1999.
- [12] Srinivas, S., Gayathri, R. and Kothandapani, M., "The influence of slip conditions, wall properties and heat transfer on MHD peristaltic transport", *Computer Physics Communications* 180, 2115-2122, 2009.



- [13] Hayat, T., Javad, M. and Ali, N., "MHD peristaltic channel flow of a Jeffrey fluid with compliant walls and porous medium", *Transport Porous Media* 74, 243-259, 2008.
- [14] Derek, C., Tretheway, D.C. and Meinhart, C.D., "Slipflow on peristaltic transport", *Physics and Fluids* 14, 23-43, 2002.
- [15] Hron, J., Roux, C.L., Malik, J. and Rajagopal, K.R., "Analytical solutions for the flows of a generalized fluid of complexity two in special geometries", *Computer and Mathematics Applied* 56, 2113-2128, 2008.
- [16] Kwang-Hua, W. C. and Fang, J., "Peristaltic transport in a slip flow", *The European physical Journal* 16, 511- 513, 2000.
- [17] Sud, V.K., Sekhon, G.S., Mishra, R.K., "Effect of a moving magnetic field on blood flow", *Mathematics and Biology* 39, 373-385, 1977.
- [18] Ebaid, A., "MHD and wall slip conditions on the peristaltic transport of a Newtonian fluid in an asymmetric channel", *Physics Letter A* 372, 4479-4493, 2008.
- [19] Radhakrishnamacharya, G., Srinivasulu, Ch. and Mecanique, C. R., "Interaction of peristalsis with heat transfer for the motion of a viscous incompressible Newtonian fluid in a channel with wall effects", *CRMechanique* 335, 348-369, 2007.
- [20] Nadeem, S. N. and Akbar, S., "MHD peristaltic flow of an incompressible Newtonian fluid in a uniform channel with variable viscosity in the presence of heat transfer analysis", *Communication Nonlinear Science Numerical Simulation* 14, 3836-3844, 2009.
- [21] Kothandapani, M. and Srinivas, S., "Influence of elasticity of the flexible walls on the peristaltic motion of a MHD fluid in a porous medium with heat transfer", *Physics Letter A* 372, 4572-4586, 2008.
- [22] Radhakrishnamacharya, G. and Srinivasulu, Ch., "Influence of wall properties on peristaltic transport with heat transfer", *CRMechanique* 335, 369-373, 2007.
- [23] Taneja, R. N. and Jain, C., "MHD free convection flow in the presence of a temperature dependent heat source in a viscous incompressible fluid in vertical channel", *Deferent Science Journal* 54, 1-21, 2004.
- [24] Vajravelu, K., Radhakrishnamacharya, G. and Radhakrishnamurthy, V., "Peristaltic flow and heat transfer in a vertical porous annulus, with long wave approximation", *International Journal Non-Linear Mechanics* 42, 754-759, 2007.





- [25] Mekheimer, KH. S. and Abdelmaboud, Y., "The influence of heat transfer and magnetic field on peristaltic transport of a Newtonian fluid in a vertical annulus: Application of an endoscope", *Phys Letter A* 372, 1657-1665, 2008.
- [26] Drew, D.A., "Stability of Stokes Layer of a Dusty Gas", *Physics and Fluids* 19, 2081-2084, 1979.
- [27] Charm, S.E. and Kurkland, G.S., "Blood flow and microcirculation", John Wiley Newyork, 1974.
- [28] Tam. C. K. W., "The drag on a cloud of spherical particles in low Reynolds number flow", *Journal Fluid Mechanics* 38, 537-546, 1969.